Available online at www.sciencedirect.com
SCIENCE DIRECT®
Solar Energy Materials & Solar Cells
ELSEVIER
Solar Energy Materials & Solar Cells 86 (2005) 517–526
www.elsevier.com/locate/solmat

Optimisation of interdigitated back contacts solar cells by two-dimensional numerical simulation

O. Nichiporuk[a,b], A. Kaminski[a,*], M. Lemiti[a], A. Fave[a], V. Skryshevsky[b]

[a] *Laboratoire de Physique de la Matière, Inst. Nat. des Sci. Appliquees Lyon, UMR-CNRS 5511, Bât. Blaise Pascal, 7 Avenue Jean Capelle, Villeurbanne Cedex 69621, France*
[b] *Radiophysics Department, National Taras Shevchenko University, 64 Vladimirskaya, Kiev 01033, Ukraine*

Received 4 February 2004; accepted 7 September 2004
Available online 11 November 2004

Abstract

In this paper we present the results of the simulation of interdigitated back contacts solar cell on thin-film (~50 μm) silicon layer. The influence of several parameters (surface recombination rate, substrate thickness and type, diffusion length, device geometry, doping levels) on device characteristics are simulated using the accurate two-dimensional numerical simulator DESSIS that allows to optimise the cell design.

Keywords: Interdigitated back contacts; Simulation; Thin film

1. Introduction

A key question that remains in photovoltaic production is the cell cost. One of the promising ways of reducing this cost is by reducing the direct material cost, e.g. by the application of thin film technologies. Recently, the interest to interdigitated back contact solar cells (IBC SC) has been arisen due to several advantages of these cells [1–3]. Indeed, compared to the routine p–n junction solar cells, the IBC SC can have

*Corresponding author. Tel.: +33 4 72 74 85 40; fax: +33 4 7243 8531.
E-mail addresses: chip@univ.kiev.ua (O. Nichiporuk), annek@insa-lyon.fr (A. Kaminski).

0927-0248/$ - see front matter
doi:10.1016/j.solmat.2004.09.010

lower series resistance (there is no need to conduct current along emitter and the metallization pattern can cover the whole cell surface), improved optical confinement (no grid shading loss) and simplicity for the solar cells interconnection into modules (co-planar interconnection). Moreover, because of the low series resistance R_s, IBC SC is more efficient under operation at concentrated solar illumination [4].

Since p–n junction and ohmic terminals lie on the non-illuminated side of the cell, the charge carriers photogenerated nearby front surface pass across the bulk of the cell. Therefore, both the front surface recombination velocity and the diffusion length of minority charge carriers are the ultimate parameters controlling the cell efficiency. The optimisation of the IBC SC based on Si wafers of high electronic quality ($\tau = 1$ ms, $L_D \approx 1500$ μm, $S_0 = 100$ cm/s) was performed [5]. The simulated efficiency limit for IBC SC can reach 24.3% [6]. SunPower Corporation produces Pegasus interdigitated back-contacts solar cells on 160 μm thick FZ n-type silicon substrate with typical efficiency of 22.5% operating under one-sun illumination [1].

Recently, the method of epitaxial layer transfer [7,8] has been developed to create thin (~50 μm) epitaxial silicon films on foreign substrates. Elaborated epitaxial p-type silicon films show an electron diffusion length up to $L_D = 100$–300 μm [9]. Such films can be regarded as promising for IBC cells realisation. Therefore, the optimisation of IBC solar cells based on epitaxial silicon film on foreign substrate and with lower lifetime than high-quality FZ silicon substrate is a topical question.

To optimise the IBC SC design, 2D or 3D numerical simulations are applied. In fact, n^+ and p^+ regions are placed on one side of the cell toward each other, which requires the consideration of 3D current flows. There are a large number of parameters that describe the cell during numerical simulation (width of doped n^+ and p^+ regions, depth and level of doping, distance between diffused regions, substrate thickness and doping level and profile, diffusion length, back and front surface recombination rates and optical parameters of front and back surfaces).

In this paper we present 2D numerical simulation of IBC SC on thin silicon film with L_D in the range 200–300 μm which corresponds to values obtained on epitaxial layers grown on porous silicon [9]. Moreover, the dimensions chosen for contacts geometry correspond to a potential industrial application of the interdigitated solar cell technology with screen-printed contacts. As simulation parameters, we select the surface recombination rate, diffusion length, doping level and type of the substrate, p^+ and n^+ regions, geometrical dimensions of n^+ and p^+ regions and substrate thickness.

2. Simulated models and structure

For numerical simulation of IBC SC, the software package DESSIS, part of the modelling tools pack ISE TCAD 8.5 is used. It incorporates advanced physical models and robust numerical methods for the 2D simulation of semiconductor devices [10]. Because of the periodicity of IBC SC structure, a reference cell element was chosen for the simulation. A general view of the simulated structure with a p-type wafer is shown in Fig. 1.

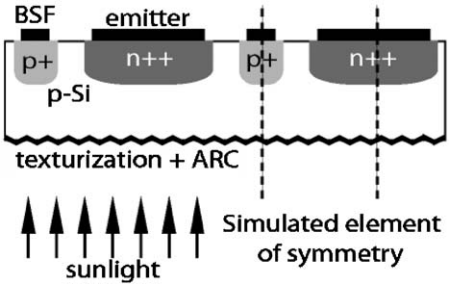

Fig. 1. Cross section of investigated structure and the elementary cell used for simulations (for a n-type structure, the reference cell is the same with inverted doping types).

Table 1
Parameters used for the reference solar cell

Parameter	Value
Base	
Thickness	50 μm
Type	p or n
Doping (N_A or N_D)	$10^{16}\,cm^{-3}$
Diffusion length (L_d)	200 and 300 μm
BSF	
Doping (N_D or N_A)	$5\times10^{19}\,cm^{-3}$
Thickness	1 μm
Profile	Complementary error function
Half-width	25 μm
Emitter	
Doping (N_D or N_A)	$10^{20}\,cm^{-3}$
Thickness	0.6 μm
Profile	Complementary error function
Half-width	50 μm
Spacing between BSF and emitter	25 μm
Optical confinement	
Front	SiN 70 nm, texturised with an angle of 54.7°
Back reflectivity	0.9
Surface recombination	100 cm/s (front and back)

For the simulation of IBC cell, we use the following models: Shockley–Read–Hall (SRH) recombination model, band gap narrowing [11–13], dependence of the lifetimes with doping level [14–16], Auger recombination [17–19], doping-dependent mobility model [20–22], AM1.5 G solar spectrum [23].

The reference cell parameters are given in Table 1.

In this structure, the contacts cover the whole doped region area. This is not the optimal solution for the improvement of the efficiency because of the high

Table 2
Efficiency obtained on the reference solar cell

	Efficiency (%) n-type substrate	Efficiency (%) p-type substrate
$L_D = 200\,\mu m$	17.85	18.43
$L_D = 300\,\mu m$	18.52	19.26

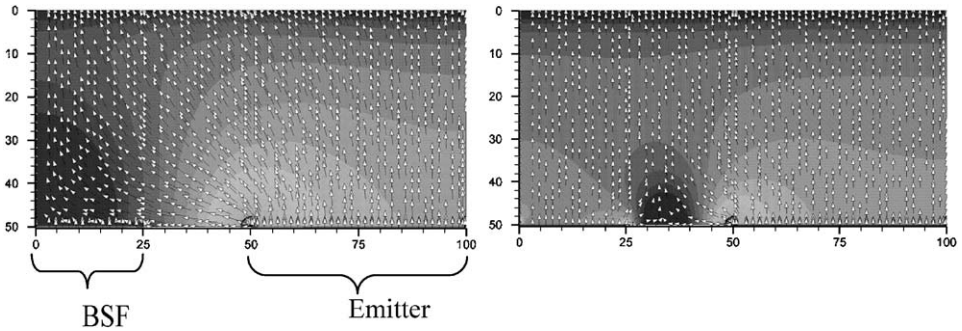

Fig. 2. Left: Electron current flow for p-type substrate, $Lp = 300\,\mu m$ and BSF doping $= 5 \times 10^{19}\,cm^{-3}$ (BSF from 0 to 25 μm), efficiency = 19.26%. Right: Same simulated structure but with a BSF doping of $10^{17}\,cm^{-3}$ (efficiency = 12.76%).

recombination rate at the contacts interface. However, this permits to use a simplified technological process for industrial applications like, for instance, self-doped screen-printed contacts [24] or self-aligned process [25]. An alternative to reduce the recombination at the contact interface is the MIS structure proposed by Muller et al. [26].

The efficiency obtained on the reference solar cell is presented in Table 2.

The lower efficiencies obtained on n-type substrates with similar diffusion length than p-type substrate are due to the difference of mobility between electron and holes in silicon. Since electron mobility is three time higher than holes mobility, higher quality n-type silicon is necessary to obtain similar efficiency than p-type silicon. This is possible due to the absence of boron–oxygen complexes in n-type silicon and lower recombination activity of transition metals [27].

2D simulation is more suitable for interdigitated solar cells optimisation than 1D simulation because the lines of the current flow are not perpendicular to front and back surfaces. For example, minority carriers generated above the back-surface field (BSF) must reach the p-n junction to be collected. This distance can be higher than the substrate thickness. Moreover, in 1D simulation, it is difficult to simulate back surface recombination between BSF and emitter, recombination at the BSF contact and BSF influence. To illustrate this point, we have presented in Fig. 2, the electron current flow for two different BSF (p^+) doping levels.

3. Results and discussion

Fig. 3 shows cell efficiency and open-circuit voltage versus substrate doping level. As one can see, the optimal value of substrate doping is near $10^{16}\,cm^{-3}$. For less substrate doping level, V_{oc} drops because the recombination at the contact increases due to the lower built-in potential of the p–n junction (this leads to a less effective barrier for minority carriers). On the other hand, with higher substrate doping level, the increasing of bulk recombination rate leads to the decreasing of photocurrent. For doping levels above $10^{16}\,cm^{-3}$, the photocurrent decreasing becomes more important compared to the increase of p–n junction built-in potential and the cell efficiency sharply drops from about 19.5% at $10^{16}\,cm^{-3}$ to about 1% at $10^{18}\,cm^{-3}$. The drastic drop of the efficiency illustrates one of the main differences between back contacted and both sides contacted solar cells. In IBC solar cells, generated carriers at the front surface have to cross the cell to be collected whereas in two sides contacted solar cells, most of the carriers are generated near the front surface that is to say near the p–n junction.

Fig. 4 shows the cell efficiency and V_{oc} versus emitter doping level. As can be seen, the emitter doping level does not strongly influences the cell efficiency if it is above

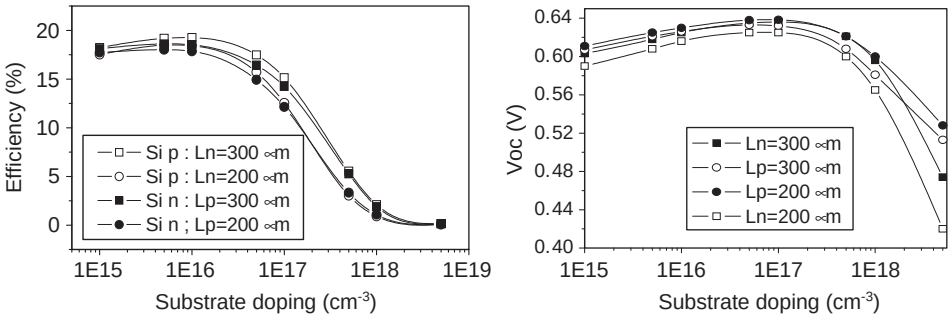

Fig. 3. Cell efficiency and open-circuit voltage versus substrate doping level.

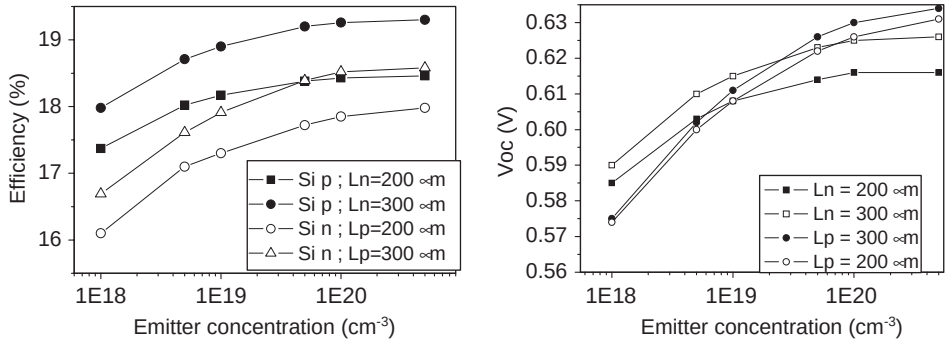

Fig. 4. Cell efficiency and open-circuit voltage versus emitter doping level.

$10^{19}\,cm^{-3}$. One can consider that the photogeneration and recombination in the emitter is very small due to the small emitter thickness (0.6 μm in comparison with a total cell thickness of 50 μm) and emitter position at the non-illuminated side of the cell. Therefore, recombination processes in the emitter region practically do not change the cell efficiency. On the other hand, emitter doping below $10^{19}\,cm^{-3}$ leads to a decrease of the p–n junction built-in potential and degradation of the cell performances.

The cell efficiency versus diffusion length for different substrate thickness W is shown in Fig. 5.

In order to eliminate efficiency dropping with cell thickness, it is necessary to bring in correspondence the geometry and substrate electronic quality: the distance between any point of photogeneration in the cell and the junction should be much less than the diffusion length ($L_D/W > 3$–4). Therefore, for a 50 μm thick cell, wholly satisfactory diffusion length of epitaxial Si is about 200 μm, whereas for a 150 μm thick cell, a diffusion length of 300 μm is insufficient (Fig. 5). As can be seen in Fig. 5, the low diffusion length and lifetime dramatically make worse the cell yield. Hence, the high electronic quality of the epitaxial layer issues the IBC solar cell parameters.

Another key parameter that controls the efficiency is the surface recombination rate. The front surface recombination is more important for IBC cell efficiency than back surface recombination (Fig. 6). However for surface recombination rates lower than 100 cm/s, the efficiency variation is small.

2D simulation also allows optimising the planar geometry of IBC solar cells. Fig. 7 shows IBC cell efficiency versus emitter and BSF thickness. As can be seen in Fig. 7, a thickness of 1–2 μm for n^+ emitter and p^+ BSF regions leads to good efficiencies. The recombination at the n^+ emitter and p^+ BSF is very small due to their placement at the non-illuminated side of the cell. To explain the efficiency increase with the emitter thickness we have analysed the electron and hole components of the emitter current. With the decreasing of the emitter thickness the photogenerated electron current does not change significantly whereas the dark hole current increases drastically for an emitter thicknesses less than 1 μm. This increasing of the dark current can be explained by the influence of the recombination rate at the

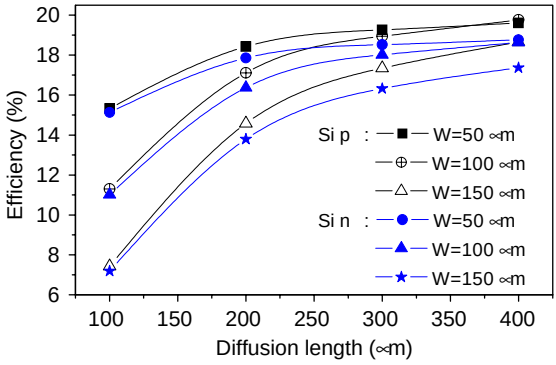

Fig. 5. Cell efficiency versus diffusion length for different substrate thickness W.

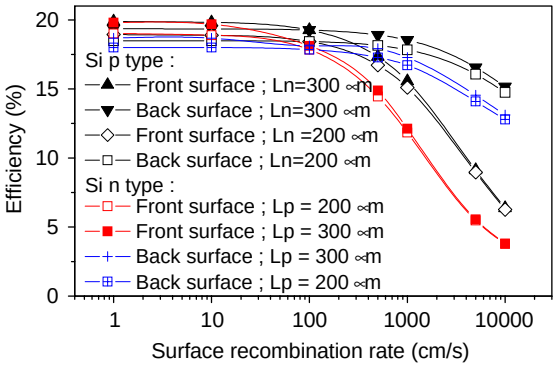

Fig. 6. Cell efficiency versus front and back effective surface recombination rates for AM1.5 G spectra.

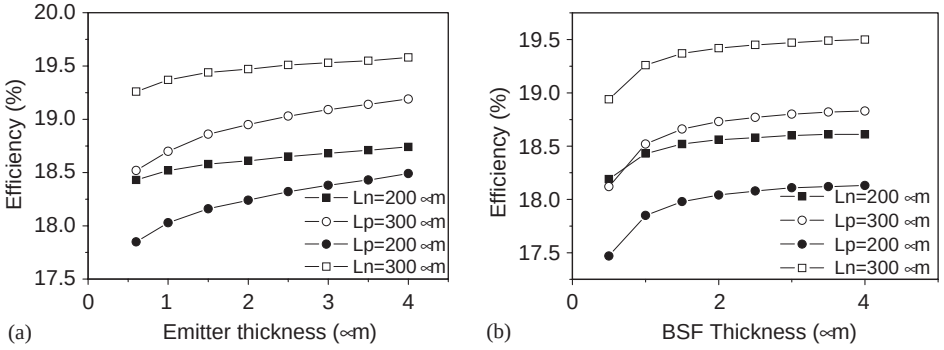

Fig. 7. (a) (left) Cell efficiency versus emitter thickness; (b) (right) cell efficiency versus BSF thickness.

contact. To justify this assumption we have performed a 1D simulation with PC1D [28] (Fig. 8). The dark current through the biased p–n junction was analysed (for $V_{bias} = 0.7$ V) for the two following cases:

(1) strong recombination at the emitter surface (in this case, the ohmic contact covers the whole surface of the emitter);
(2) no recombination at the emitter surface (in this case, the emitter is well passivated and the ohmic contact covers only a small part of the emitter).

In Fig. 8, we can see that a strong recombination at the contact leads to the increase of the dark current with decreasing of the emitter thickness. The same explanation (increase of the recombination at the ohmic contact with decreasing of the doped region thickness) can be applied for the variation of the efficiency versus BSF thickness dependencies.

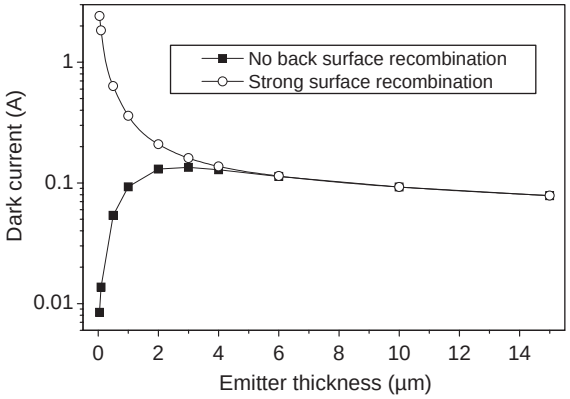

Fig. 8. Dark emitter current at 0.7 V in the case of strong back surface recombination rate at the contact and in the case of well-passivated emitter surface (PC1D simulation).

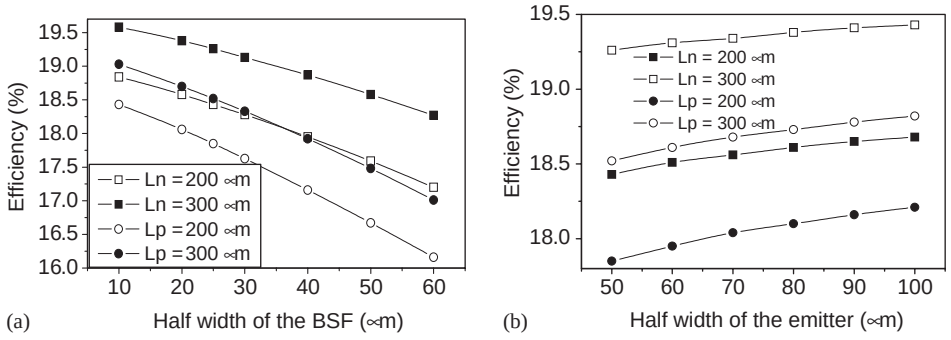

Fig. 9. (a) (left) Cell efficiency versus BSF width; (b) (right) cell efficiency versus emitter width.

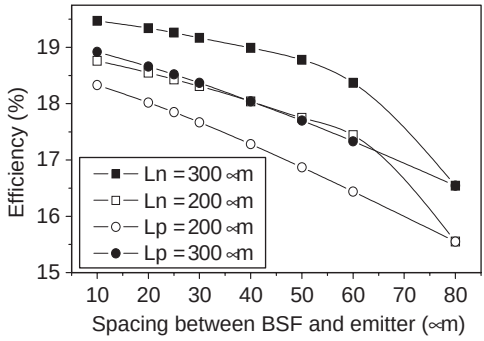

Fig. 10. Cell efficiency versus spacing between diffused back regions.

Fig. 9 illustrates the efficiency variation versus emitter and BSF width. The emitter width must exceed the BSF width 2–3 times independently from the distance between n^+ and p^+ regions.

Fig. 10 presents the variation of the efficiency versus spacing between emitter and BSF regions. The smaller the width, the higher the efficiency is because the recombination of minority carriers on the surface between emitter and BSF is smaller.

4. Conclusion

In this study, we have simulated interdigitated back contact solar cells realised on n- and p-type wafers with a diffusion length of 200 or 300 μm. 2D numerical simulations with DESSIS software package allows us to study the influence of geometry, doping, recombination, optical constants and other parameters on cell efficiency. The results obtained for our reference cell can be applied to the realisation of interdigitated solar cells on epitaxial layers transferred on a low cost substrate. Moreover, the dimensions of our simulated structure are adapted to an industrial screen-printing process and can be used to optimise an industrial development. We have also demonstrated better efficiencies on p-type substrates than on n-type substrates due to higher electron mobility (and therefore higher hole lifetime for a same diffusion length). However, n-type substrates present the advantage of better surface passivation [29], the absence of boron–oxygen complexes and lower recombination activity of transition metal impurities [27]. Therefore, very good efficiencies can be obtained on this type of substrates [1].

References

[1] R. McIntosh, M.J. Cudzinovic, D.D. Smith, W.P. Mulligan, R.M. Swanson, 19th EPVSEC, Paris, France, 2004.
[2] R. Hezel, Novel back contact silicon solar cells designed for very high efficiencies and low-cost mass production, 29th IEEE PVSC, New Orleans, Louisiana, 2002.
[3] J.G. Fossum, A. Neugroschel, F.A. Lindholm, Solid State Electron. 23 (1980) 1127–1138.
[4] M. Boumaour, F. Van de Weile, Electron. Lett. 20 (23) (1984) 949–950.
[5] D.J. Chin, D.H. Navon, Solid State Electron. 24 (1981) 109–114.
[6] Hiroyuki Ohtsuka, Yasuyuki Ohkura, Tsuyoshi Uematsu, Terunori Warabisako, Prog. Photovoltaics: Res. Appl. 2 (1994) 275–285.
[7] N. Sato, K. Sakaguchi, K. Yamagata, Y. Fujiyama, J. Nakayama, T. Yonehara, Jpn. J. Appl. Phys. 35 (1996) 973–977.
[8] R.B. Bergmann, T.J. Rinke, R.M. Hausner, M. Grauvogl, M. Vetter, J.H. Werner, Int. J. Photoenergy 1 (1999) 89–93.
[9] A. Fave, J. Kraiem, S. Quoizola, A. Kaminski, M. Lemiti, A. Laugier, 3rd WCPVSEC, Osaka, Japan, 2003.
[10] P.P. Altermatt, G. Heiser, T. Kiesewetter, K.R. McIntosh, C.B. Honsberg, S.R. Wenham, M.A. Green, 26th IEEE PVSC, Anaheim, CA, 1997, pp. 179–182.
[11] S.M. Sze, Semiconductor Devices, Physics and Technology, Wiley, New York, USA, 1985 564pp.
[12] J. del Alamo, S. Swirhun, R.M. Swanson, Solid State Electron. 28 (1–2) (1985) 47–54.

[13] M.A. Green, J. Appl. Phys. 67 (6) (1990) 2944–2954.
[14] J.G. Fossum, Solid State Electron. 19 (1976) 269–277.
[15] J.G. Fossum, D.S. Lee, Solid State Electron. 25 (8) (1982) 741–747.
[16] J.G. Fossum, R.P. Mertens, D.S. Lee, J.F. Nijs, Solid State Electron. 26 (6) (1983) 569–576.
[17] L. Huldt, N.G. Nilsson, K.G. Svantesson, Appl. Phys. Lett. 35 (10) (1979) 776–777.
[18] W. Lochmann, A. Haug, Solid State Commun. 35 (1980) 553–556.
[19] R. Häcker, A. Hangleiter, J. Appl. Phys. 75 (1994) 7570–7572.
[20] G. Masetti, M. Severi, S. Solmi, IEEE Trans. Electron Devices ED-30 (1983) 764–769.
[21] C. Canali, G. Majni, R. Minder, G. Ottaviani, IEEE Trans. Electron Devices ED-22 (1975) 1045–1047.
[22] D.M. Caughey, R.E. Thomas, Proc. IEEE (1967) 2192–2193.
[23] A.K. Rajkanan, R. Singh, J. Shewchun, Solid State Electron. 22 (1979) 793–795.
[24] D.L. Meier, H.P. Davis, P. Hacke, R.A. Garcia, S. Yamanaka, S. Salami, J.A. Jessup, 17th EPVSEC, Munich, Germany, 2001, pp. 1323–1326.
[25] R.A. Sinton, R.M. Swanson, IEEE Trans. Electron Devices ED-37 (1990) 348–352.
[26] J.W. Müller, A. Merkle, R. Hezel, 19th EPVSEC, Paris, France, 2004.
[27] J. Libal, T. Buck, R. Kopecek, P. Fath, K. Wambach, M. Acciarri, S. Binetti, L.J. Geerligs, 19th EPVSEC, Paris, France, 2004.
[28] PC1D version 4.4 for Windows, University of South Wales, Australia, 1996.
[29] A. Moehlecke, C. Del Canizo, I. Zanesco, A. Luque, 2nd WCPVSEC, Vienna, Austria, 1998, pp. 1551–1554.